NASA TECHNICAL NOTE

NASA TN D-2544

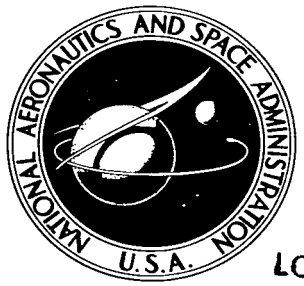

NASA TN D-2544

A PARAMETRIC EXPLORATION OF AXIAL-FLOW TURBINES FOR RANKINE CYCLE SPACE POWERPLANTS IN THE MEGAWATT RANGE

by John L. Klann and Paul T. Kerwin

Lewis Research Center

Cleveland, Ohio

NATIONAL AERONAUTICS AND SPACE ADMINISTRATION • WASHINGTON, D. C. • DECEMBER 1964

A PARAMETRIC EXPLORATION OF AXIAL-FLOW TURBINES FOR RANKINE CYCLE SPACE POWERPLANTS IN THE MEGAWATT RANGE

By John L. Klann and Paul T. Kerwin

Lewis Research Center
Cleveland, Ohio

NATIONAL AERONAUTICS AND SPACE ADMINISTRATION

For sale by the Office of Technical Services, Department of Commerce,
Washington, D.C. 20230 -- Price $0.75

A PARAMETRIC EXPLORATION OF AXIAL-FLOW TURBINES FOR RANKINE CYCLE SPACE POWERPLANTS IN THE MEGAWATT RANGE

by John L. Klann and Paul T. Kerwin

Lewis Research Center

SUMMARY

A parametric analysis has been conducted to determine the interactions of several design variables in obtaining maximum turbine efficiency. Alkali-metal vapor, axial-flow turbines were investigated within a framework of several generalizing assumptions. Efficiency reductions due to the presence of moisture have not been included. Trends rather than magnitude were emphasized.

Turbine tapering (i.e., changing the ratio of last- to first-stage blade mean-section diameter) was an effective means for attaining maximum overall static efficiency with a minimum number of stages. The turbine taper ratios for maximum efficiency solutions decreased with increasing working fluid molecular weights. At an inlet temperature of 2500° R, these solutions were characterized by 12 stages for sodium with a taper ratio of at least 1.5, 7 stages for potassium with a taper ratio of roughly 1.3, 5 stages for rubidium with a taper ratio of 0.985 (nearly constant mean diameter), and 3 stages for cesium with a taper ratio of 0.95 (nearly constant tip diameter).

Changes in turbine taper ratio and/or changes in stator exit angles were shown to be a possible means for providing wide margins of selection in design rotational speed, while still maintaining a high level of efficiency. The advantages of turbine tapering in reducing the number of stages required for nearly maximum efficiency were shown to decrease with decreasing inlet temperature. The obtainable maximum efficiency decreased with decreasing ratios of outlet to inlet temperature. Hence, selection of a low ratio of outlet to inlet temperature may penalize turbine and system performance.

Over a generator power output level from 1 to 10 megawatts, it was found that turbine diameter and rotational speed could be scaled directly within an error of ±2 percent, independent of any prescribed turbine taper ratio and number of stages. Two working fluid states were investigated. Ramifications of the choice of disk taper ratio limit, last-stage hub-to-tip radius ratio, blade-root stress correction factor, and small changes in assumed stress level were explored.

INTRODUCTION

Turboelectric propulsion is currently being considered for future space missions. In this type of system, nuclear energy is converted to mechanical energy in a high-temperature Rankine cycle using an alkali metal as the working fluid. The turbine in this cycle drives an alternator, which produces the electrical energy that is used for propulsion. One requirement of such systems is low specific powerplant weight.

Although the turbine is comparatively light (see ref. 1), its performance has a direct effect on the size of the radiator and, therefore, on the weight of the system. The gross effects of turbine inlet temperature and efficiency on required radiator area are shown in reference 2. For example, a 200° increase in inlet temperature reduces radiator area by about 30 percent, while a 10-percent decrease in efficiency increases the required radiator area by about 15 percent. This reference also contains an estimate of the number of stages required to achieve high efficiency with a stage speed-work parameter of 0.5 for working fluids of rubidium, potassium, and sodium. Reference 3 presents a more detailed look at turbine characteristics at the 1-megawatt power level. The efficiency correlation of reference 4 is used to show the minimum number of stages required to obtain a level of at least 0.8 in aerodynamic efficiency. It is also shown in reference 3 that the use of increasing rather than constant blade mean-section diameters from the first to the last stage results in fewer required stages.

The purpose of this investigation was to take a more detailed look at the turbine as one of the Rankine cycle system components. In general, the turbine designer may select among many geometric parameters to best fit the thermodynamic requirements for each particular application. On the other hand, the systems engineer must specify the thermodynamic constraints to best fit the overall powerplant requirements. Both of these problems have been investigated; emphasis was placed on obtaining nearly maximum turbine efficiency and a parametric exploration of the trade-offs in turbine design, which may be available in the cycle-selection process. Although the analysis is not intended as a design procedure, it is general enough to demonstrate design trends.

In the analysis, aerodynamic efficiency has been retained as a dependent variable. The correlation of reference 4 has been employed, and the effects of moisture on efficiency has been neglected. Efficiency reductions due to the presence of moisture are recognized, but adequate data are not available to predict their magnitude. It was assumed that the losses due to moisture will not be changed much by the variations investigated and that trends in "aerodynamic" efficiency will reflect the trends in overall efficiency.

An IBM 7094 computer was employed to determine the effects of geometry, inlet temperature, temperature ratio, stress level, power level, and the working fluid on axial-flow turbines.

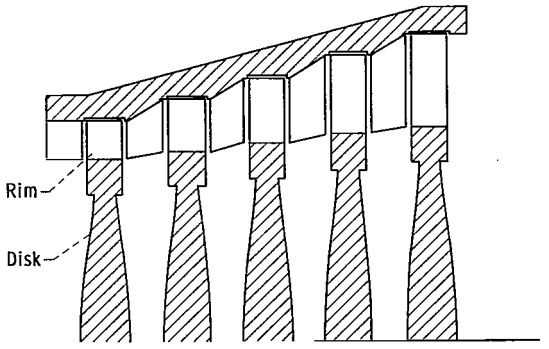

Figure 1. - Analytical turbine model.

METHOD OF ANALYSIS

A sketch of the turbine model is shown in figure 1. Conceptually, it is a conventional multistage turbine; the blades of each wheel are attached to square rims, with the disks shaped for constant stress. One of the main geometrical variations was stage-to-stage blade mean-section diameter. Symbols are defined in appendix A, while details of the analytical technique are presented in appendix B. In order to calculate the required turbine work and weight flow, the overall turbine and generator efficiencies were assumed to be 0.8 and 0.9, respectively. Efficiency reductions due to moisture were not evaluated, but the assumption of an overall turbine efficiency of 0.8 was an attempt to account for these losses.

For the purposes of this investigation, a set of reference values has been chosen and is presented in table I. Each of these parameters is discussed to bring some of the generalizing assumptions to the reader's attention.

Working Fluid

Arbitrarily, potassium has been employed as the basis for exploring variations in the other turbine parameters; however, the effects of cesium, rubidium, and sodium on turbine performance characteristics have also been investigated.

TABLE I. - REFERENCE VALUES AND RANGES OF TURBINE PARAMETERS INVESTIGATED

Parameter	Reference value	Other values investigated
Working fluid	Potassium	Cesium, rubidium, and sodium
Inlet temperature, T_i, $^{\circ}R$	2500	2400 and 2300
Turbine taper ratio, $D_{m,n}/D_{m,1}$	1.0	0.8 to 1.5
Temperature ratio, T_o/T_i	0.772 to 0.778	0.65 to 0.85
Allowable stress, σ_a, percent of rupture stress	50	40 and 60
Inlet quality, X_i	1.0	----------
Last-stage hub-to-tip radius ratio, $(r_h/r_t)_n$	0.7	0.6 to 0.8
Stator exit angle, α, deg	70	60 to 80
Disk taper ratio limit, $(y_a/t_d)_{max}$	2.5	2.0 to 3.0
Mean blade aspect ratio	2.0	----------
Blade-root stress correction factor, ψ	0.7	1.0
Power level, P, Mw	1	2, 5, and 10
Fluid state	"Frozen"	"Equilibrium"

Inlet Temperature

An inlet temperature of 2500° R has been assumed to be a reasonable temperature, which Rankine cycle technology may attain. The effects of reducing the inlet temperature to 2400° and 2300° R were investigated.

Turbine Taper Ratio

The turbine taper ratio, defined as the ratio of the last- to first-stage blade mean-section diameter

$D_{m,n}/D_{m,1}$, has been adopted as one of the primary variables. Overall turbine geometry was determined by satisfying the continuity equation, specifying (1) a fixed axial blade chord, (2) the last-stage hub-to-tip radius ratio $(r_h/r_t)_n$, and (3) the turbine taper ratio, and allowing the intermediate-stage diameters to vary linearly between the first- and last-stage diameters. Turbine performance will be compared to the reference taper ratio of 1 (constant mean diameter). The range of this variable included unusual turbine geometries, the last-stage mean diameter being as small as 0.8 that of the first stage, and somewhat more conventional variations, the last-stage mean diameter being as much as 1.5 that of the first stage.

Turbine Temperature Ratio

The reference values of turbine temperature ratio were those that yielded minimum specific radiator area (sq ft/kw) for the working fluids and an assumed condensing radiator (see appendix B and ref. 3). This parameter is a measure of the turbine specific work. It is important during the cycle-selection process because trade-offs between the size and weight of the radiator and the remainder of the system are heavily dependent upon this ratio. Effects of this ratio on the turbine configuration have been included.

Stress Level

The molybdenum-based alloy, containing 0.45 percent titanium and 0.07 percent zirconium (referred to as TZM), has been assumed to be the turbine material. It is felt that this material is typical of the refractory alloys that appear to be applicable. For the reference condition, 50 percent of the rupture stress over a 20,000-hour life has been used for allowable stresses. Effects of small variations (40 to 60 percent of rupture) were included in this study to indicate the sensitivity of the results to the assumed stress.

Inlet Quality

Saturated vapor was assumed at the turbine inlet. Reference 2 has shown that superheating this flow does not appear attractive because large amounts are required to substantially reduce moisture content while cycle efficiency is reduced.

Last-Stage Hub-to-Tip Radius Ratio

A value of 0.7 has been assumed for the reference condition. This was felt to be a reasonable value on the basis of existing gas turbine technology; however, variations from 0.6 to 0.8 were also included.

Stator Exit Angle

An angle of 70° has been shown to be a reasonable value for good effi-

ciency (ref. 4) and was used for most of the calculations. This value was assigned to the blade mean-section radius of the first and last stages. Intermediate-stage stator exit angles were determined from the axial velocity component, which satisfied continuity, and the tangential component, which satisfied a requirement of having a constant stage speed-work parameter. Variations in the assigned first- and last-stage values from 60° to 80° have been included in the analysis.

Disk Taper Ratio

A disk taper ratio of 2.5 is used here as a reference value. In general, this ratio should be as large as possible without causing stage spacing problems near the axis of rotation. Limits on this ratio from 2.0 to 3.0 were investigated. Each wheel was conservatively assumed to attain the total temperature of the vapor entering that stage. Each disk was then allowed to assume the value of disk taper ratio prescribed by the allowable stress and rotational speed. Hence, all disks were fully stressed and of minimum size.

Mean Blade Aspect Ratio

A single value of 2.0 has been used. In an attempt to describe reasonable turbine geometries, a fixed axial blade chord was determined for each turbine calculation. The procedure was such that the individual stage aspect ratio varied below 2.0 in the front stages and above 2.0 in the last stages (see appendix B for more details).

Blade-Root Stress Correction Factor

A value of 0.70 has been used for the reference condition. Linear variation of the blade cross-sectional area from hub to tip has been assumed. Conceptually, the airfoil thickness rather than the rectangular planform was assumed to vary. A stress correction factor of 1 has also been investigated.

Power Level

An output of 1 megawatt with an assumed generator efficiency of 0.9 has been used for the reference value. Overall system power levels up to 10 megawatts were also considered.

Fluid State

For ease of analysis, the vapor fluid state has been assumed to be "frozen" (as used in ref. 5 with varying vapor molecular weight) for the reference condition. Frozen properties are calculated in reference 5 as the sum of the contributions from the monatomic and diatomic molecules present at a given pressure and temperature. Not included is the energy required to alter the degree of equilibrium as a result of dissociation. Reference 5 also cal-

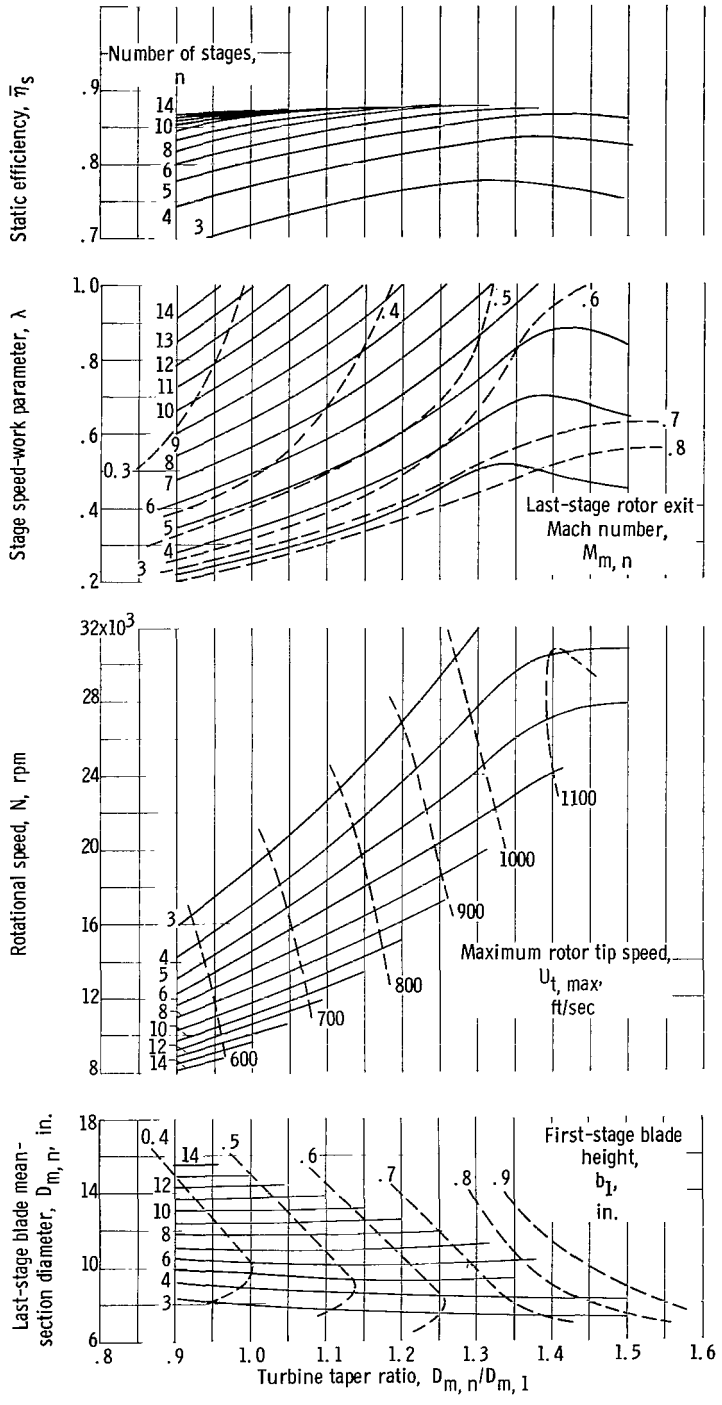

(a) Static efficiency, stage speed-work parameter, rotational speed, and last-stage blade mean-section diameter.

Figure 2. - Turbine characteristics as functions of turbine taper ratio. (See table I for reference conditions.)

culates "equilibrium" values of vapor specific heat and speed of sound, which include this energy.

The degree of dissociation occurring in the turbine expansion process is not known. In general, it is felt that the descriptive fluid state will be somewhere between the "frozen" and "equilibrium" states. Hence, for comparison, turbine characteristics using the equilibrium fluid state are also presented (see appendix B).

RESULTS AND DISCUSSION

The results of this parametric analysis are presented in two sections, namely, Geometric Variations and Thermodynamic Variations. It must be emphasized that the magnitudes shown in the results are dependent upon several generalizing assumptions. The trends and relative changes will be stressed in the discussion.

Geometric Variations

Effects of these parameters on turbine characteristics were investigated assuming potassium as the working fluid at an inlet temperature of 2500° R. Saturated vapor at the inlet and the "frozen" fluid state were assumed. The turbine temperature ratio was set at 0.772 (see appendix B), while the generator output was assumed to be 1 megawatt. (See table I, p. 3, for a complete list of reference conditions.)

Turbine tapering. - Turbine characteristics are shown in figure 2(a) as a function of turbine taper ratio $D_{m,n}/D_{m,1}$. Overall static efficiency, those

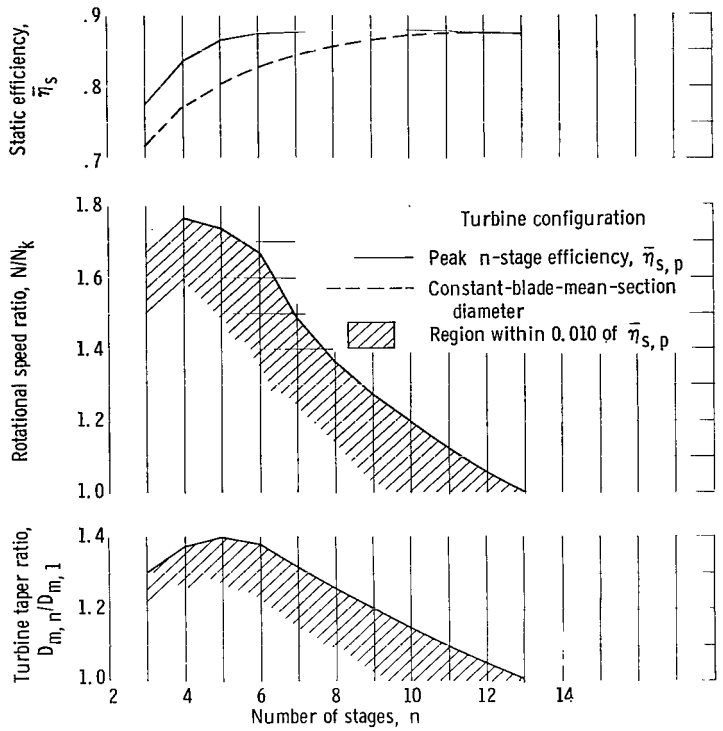

(b) Cross plot of efficiency trends.

Figure 2. - Concluded. Turbine characteristics as functions of turbine taper ratio. (See table I for reference conditions.)

values of stage speed-work parameter that satisfy the turbine specific work requirement, rotational speed, and last-stage mean diameter, are presented for 3- to 14-stage solutions. Variations of the last-stage rotor exit Mach number as calculated at the blade mean-section diameter, the maximum rotor tip speed, and the first-stage blade height are superimposed on the results.

In general, for any fixed number of stages, efficiency, stage speed-work parameter, and rotational speed initially increased as the first-stage blade mean-section diameter was decreased with respect to the last-stage blade mean-section diameter. For the three-, four-, and five-stage solutions, maximum values of efficiency and stage speed-work parameter were obtained at values of the turbine taper ratio above 1.3. Variations in last-stage mean diameter, for a fixed number of stages, were small over the range in turbine taper ratio from 0.8 to 1.5. Below turbine taper ratios of 1.3, the first-stage disks of all solutions were stress limited. Increasing the taper ratio above 1.3, for the three-, four-, and five-stage solutions moved the stress limit continuously in the turbine model, either to the blades or to the later-stage disks. Increased tapering for a fixed number of stages was accompanied by increasing rotor tip speeds, first-stage blade heights, and rotor exit Mach numbers. The latter effect was small except at large values of turbine taper ratios (above 1.3).

Figure 2(b) summarizes the effects of turbine tapering by comparing the peak efficiency solutions (or the maximum for $n > 5$, namely, those for $\lambda = 1.0$) to corresponding constant-mean-diameter solutions as a function of the number of stages. Rotational speed is divided by the n-stage constant-mean-diameter rotational speed N_k. Improved static efficiency or a reduction in the number of required stages may be obtained by permitting decreases in the first-stage diameter with respect to the last stage. For the present conditions, the largest improvement in efficiency was 0.06 for the five-stage solutions with the fifth-stage mean diameter 1.4 that of the first stage. The corresponding rotational speed was 1.735 that of the constant-mean-diameter speed. Furthermore, it may be seen that if, say, 99 percent of the maximum efficiency (0.870) were a design goal, then 11 stages would be required for a constant-mean-diameter solution as compared to six stages with tapering.

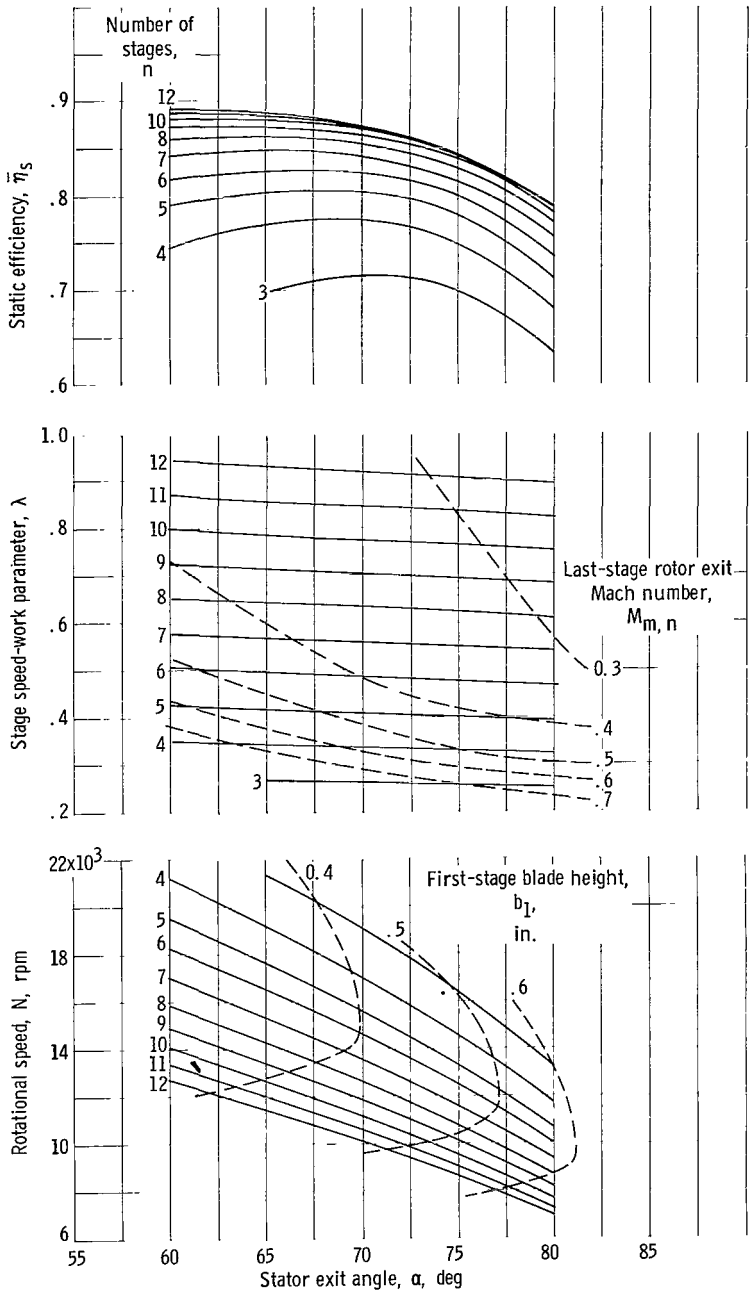

(a) Static efficiency, stage speed-work parameter, and rotational speed.

Figure 3. - Constant-blade-mean-section-diameter turbine characteristics as functions of stator exit angle. (See table I for reference conditions.)

The cross-hatched areas in figure 2(b) show a region of design variation in rotational speed and tapering available within one point of peak efficiency. It can be seen that the combined effects of tapering of the turbine flow passage and adding stages might be employed to afford good efficiency over a wide range of design rotational speeds. For example, if a static efficiency of 0.80 were acceptable, five stages for the constant-mean-diameter solutions would be required; then if tapering were permissible, rotational speed at the design point could be selected anywhere within 1.0 and 1.74 of the constant-mean-diameter speed. Of course, increasing or decreasing the number of stages would permit a still wider range in the choice of rotational speed.

Stator exit angle. - The effect of stator exit angle on the constant-mean-diameter turbine characteristics is shown in figure 3(a). Values of the stator angle that resulted in maximum static efficiency were a function of the number of stages and were characterized by decreasing angle with increasing number of stages. For any fixed number of stages, increasing the assigned stator exit angles resulted in decreasing rotational speed, stage speed-work parameter, and last-stage rotor Mach number, while the first-stage blade height increased.

Figure 3(b) summarizes the effects shown in figure 3(a). In general, the solutions for lower numbers of stages were more sensitive to stator exit angle; however, over the range from 3 to 12 stages, the reference value of 70° fell at least within 0.02 of the peak stage efficiency. Although not shown, the

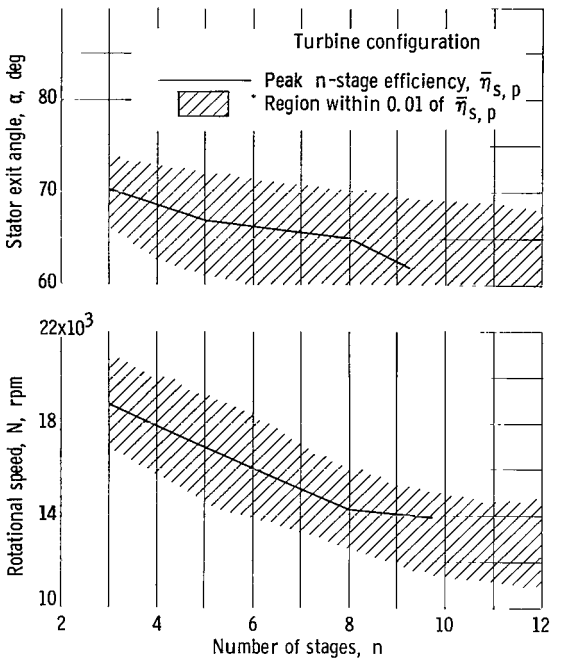

(b) Cross plot of peak efficiency trends.

Figure 3. - Concluded. Constant-blade-mean-section-diameter turbine characteristics as functions of stator exit angle. (See table I for reference conditions.)

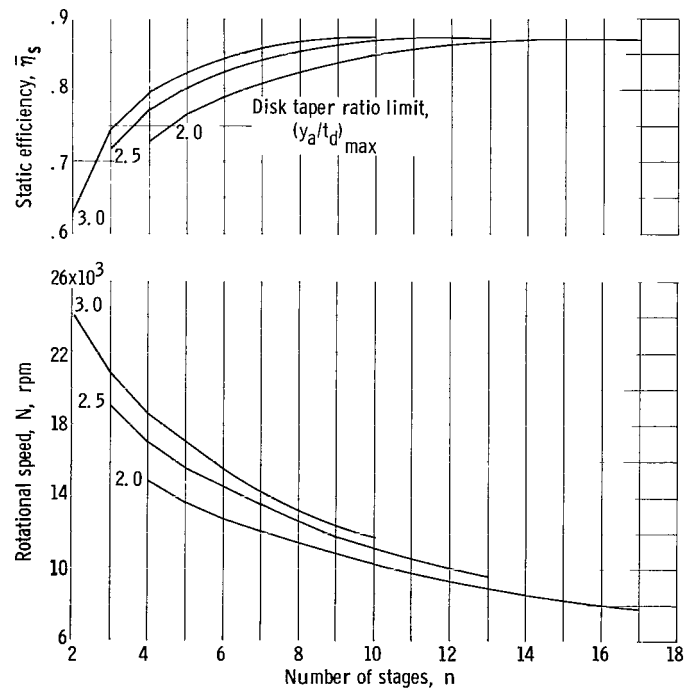

Figure 4. - Effect of disk taper ratio limit on constant-blade-mean-section-diameter turbine characteristics. (See table I for reference conditions.)

optimum stator exit angles were also functions of the turbine taper ratio, which, for a fixed number of stages increased with increasing taper ratio. Again, the solutions for lower numbers of stages were more sensitive to this effect.

Looking at this parameter in another light, it can be seen that, roughly, a $\pm 5^{\circ}$ change in stator exit angle about the optimum value can permit a ±10 percent change in design rotational speed with little penalty in efficiency.

Disk taper. - Effects of varying the disk taper ratio limit from the reference value are presented in figure 4, for constant-mean-diameter solutions. For any fixed number of stages, increasing the disk taper ratio limit resulted in increased efficiency and design rotational speed.

Again, if 99 percent of the maximum static efficiency (0.865) for constant mean-diameter turbines were set as a goal, then for the reference disk taper ratio of 2.5, nine stages would be required. Disk taper ratio limits of 3.0 and 2.0 then would result in a one-stage reduction and a four-stage increase in the number of required stages, respectively.

Last-stage hub-to-tip radius ratio. - The effects of this parameter on constant-mean-diameter turbine characteristics are presented in figure 5. For any fixed number of stages, decreasing the last-stage radius ratio resulted in increased efficiency and rotational speed.

If 99 percent of obtainable efficiency (0.867) were prescribed, then the reference last-stage radius ratio of 0.7 would require 10 stages, while a radius ratio of 0.8 would require 14 stages and a radius ratio of 0.6 would require 8 stages.

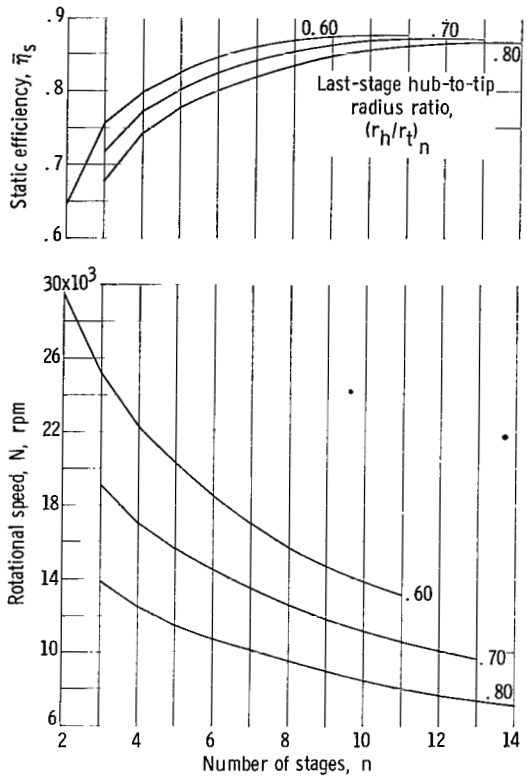

Figure 5. - Effect of last-stage hub-to-tip radius ratio on constant-blade-mean-section-diameter turbine characteristics. (See table I for reference conditions.)

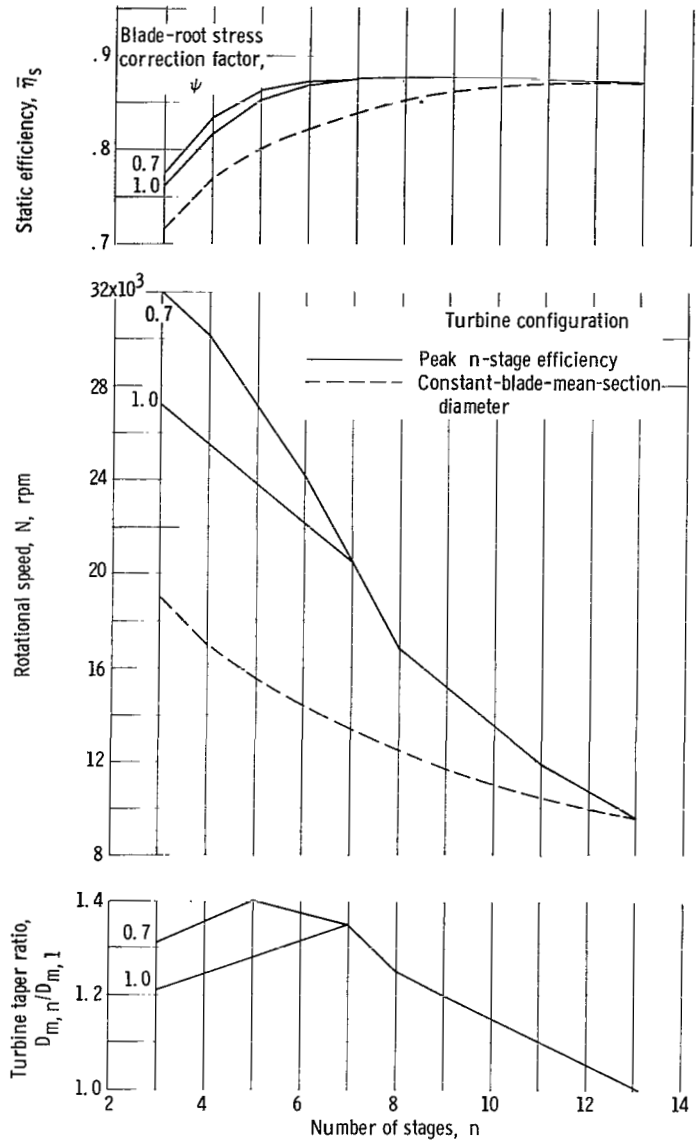

Figure 6. - Effect of blade-root stress correction factor on turbine characteristics. (See table I for reference conditions.)

Blade-root stress correction factor. - The effect of not varying the blade cross-sectional area ($\psi = 1.0$) is compared to the reference condition of $\psi = 0.7$ in figure 6. As would be expected, only those solutions that were near or at a stress limit in the blades were affected, namely, only the highly tapered, low-number-of-stage solutions ($n < 7$). For these solutions with $\psi = 1.0$, the stress limitation shifted from the disks to the blades at lower values of the turbine taper ratio. Hence, allowing the rotor blade cross-sectional areas to vary may permit increased design rotational speed and small increases (not more than 0.02) in aerodynamic efficiency for small-number-of-stage turbine designs.

Stress level. - The effect of small changes in allowable stress on turbine characteristics is summarized in figure 7. Variations for 40, 50 (the reference level), and 60 percent of the rupture stress are shown. The constant-mean-diameter solutions for any number of stages exhibited small changes in design rotational speed (roughly ±5 percent) and efficiency (within ±0.02) with the ±10 percent change in allowable stress.

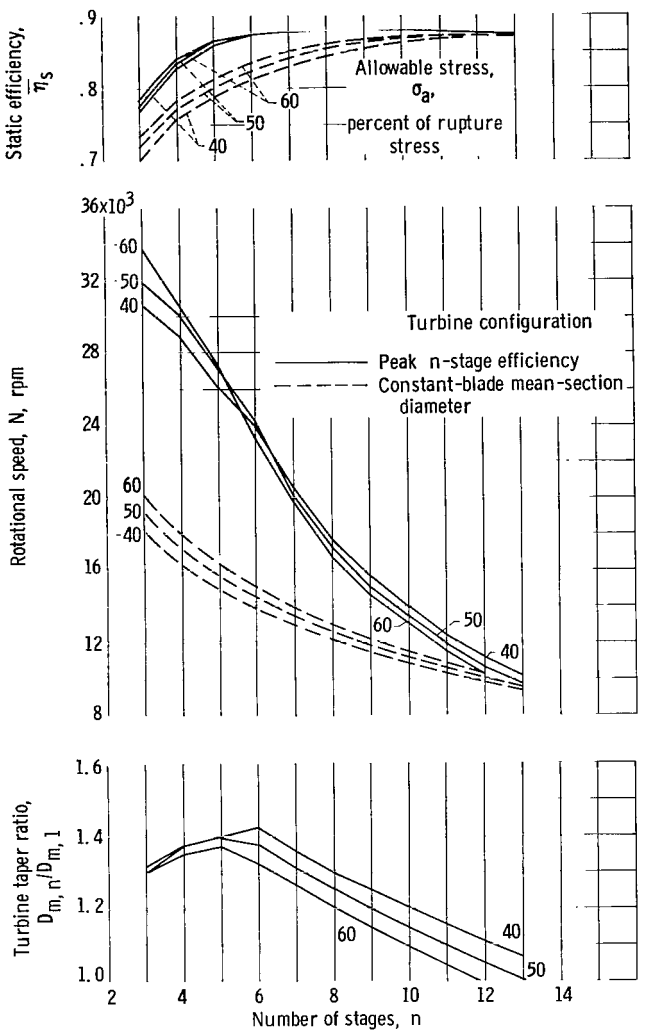

Figure 7. - Effect of stress level on turbine characteristics. (See table I for reference conditions.)

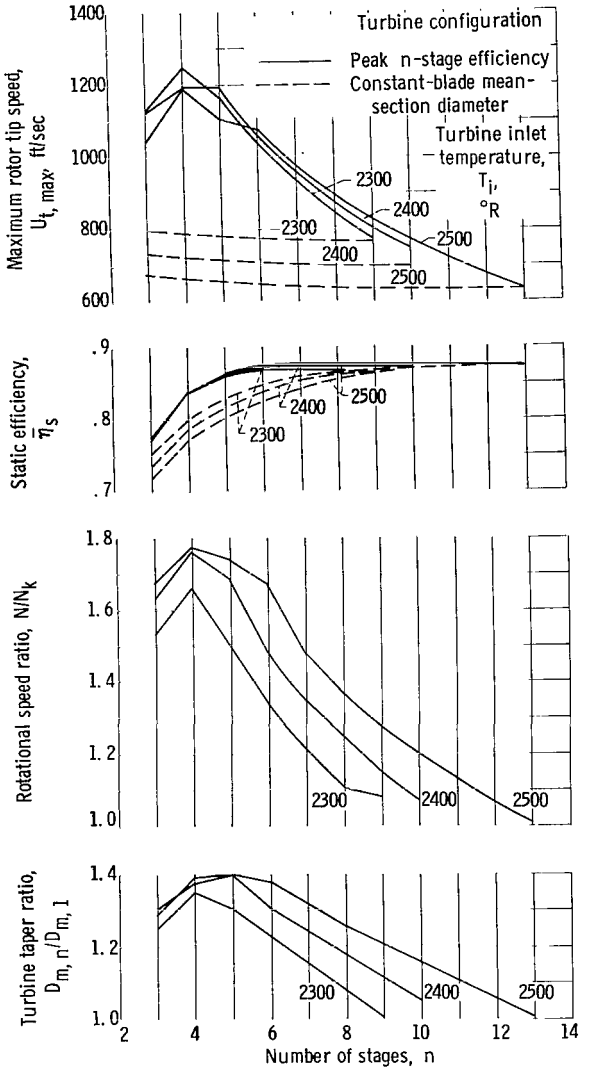

Figure 8. - Effect of inlet temperature on turbine characteristics. (See table I for reference conditions.)

The peak n-stage efficiency solutions were characterized by nonuniform variations in rotational speed with stress level for $n < 7$. The crossover among the three rotational speed curves was due to the combined effect of the varying degrees of tapering required for peak efficiency and the nonoptimum values of stator exit angles. Except for the apparent small improvements in obtainable efficiency for the three-, four-, and five-stage solutions, the small changes in allowable stress did not affect the efficiency obtainable with turbine tapering. The stress changes did, however, alter the amount of tapering required to obtain peak efficiency.

Thermodynamic Variations

Effects of these parameters on turbine characteristics were investigated

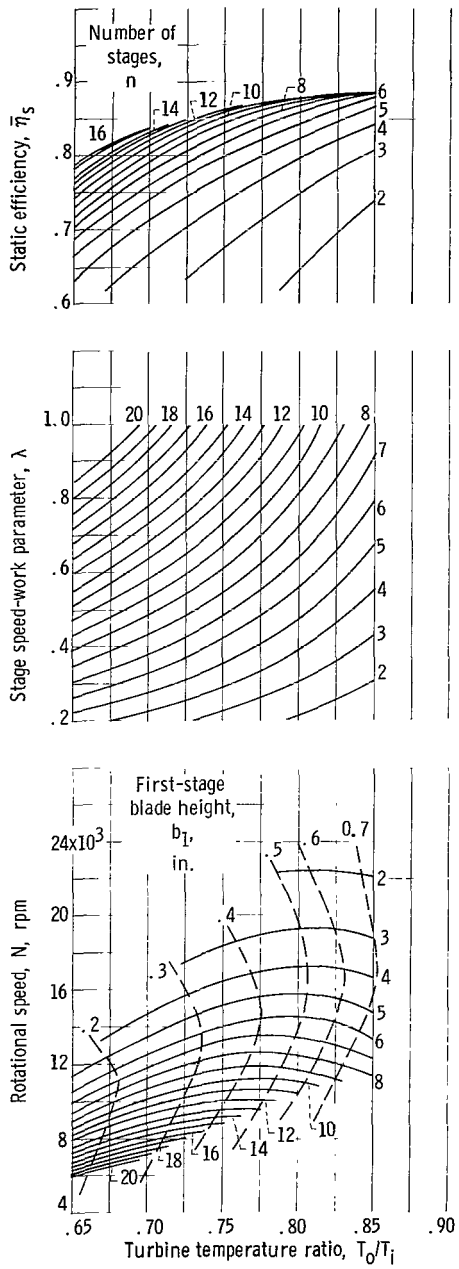

(a) Static efficiency, stage, speed-work parameter, and rotational speed.

Figure 9. - Constant-blade-mean-section-diameter turbine characteristics as functions of turbine temperature ratio. (See table I for reference conditions.)

with the reference values (see table I) of the geometrical restraints discussed previously.

Inlet temperature. - Characteristics of the turbine solutions over the range in inlet temperature from 2500° to 2300° R are summarized in figure 8. Comparison of the efficiency variations shows that, for a fixed number of stages, the improvement from constant-mean-diameter solutions to tapered turbine designs decreased with decreasing temperature. The degree of tapering (except for $n < 5$) and relative change in rotational speed required to achieve peak efficiency, however, decreased with decreasing inlet temperature. Again, the low-number-of-stage solutions exhibit less uniform variations because of their greater sensitivity to the assigned stator exit angle.

Variations in maximum rotor tip speed are included in this figure to give an indication of the relative increases due to tapering. Over this range in inlet temperature, there appears to be a narrow band of tip speeds that is a function of the number of turbine stages, which, if attained by a design, will potentially yield nearly peak efficiency.

A 0.01 decrease occurred in the maximum efficiency obtained between inlet temperatures of 2500° and 2300° R. This was largely due to a corresponding decrease in Reynolds number; however, the relative effect of inlet temperature may be compared by again setting an arbitrary goal of 99 percent of the maximum efficiency at each temperature. Then, at 2500°, 2400°, and 2300° R, the reduction in the number of required stages from the constant-mean-diameter to tapered solutions was four, three, and two, respectively. Hence, turbine tapering was more effective in reducing the number of stages required for nearly peak efficiency as inlet temperature increased.

Turbine temperature ratio. - Effects of this variable on turbine characteristics are shown in figure 9(a) for constant-mean-diameter solutions. Increasing turbine temperature ratio from 0.65 to 0.85 corresponds to decreasing the specific work by 60 percent and increasing the exit quality by 14.6 percent and required weight flow by 150 percent (see table II, p. 22). For a fixed number of stages, the aerodynamic efficiency (i.e., static) increased with increasing temperature ratio.

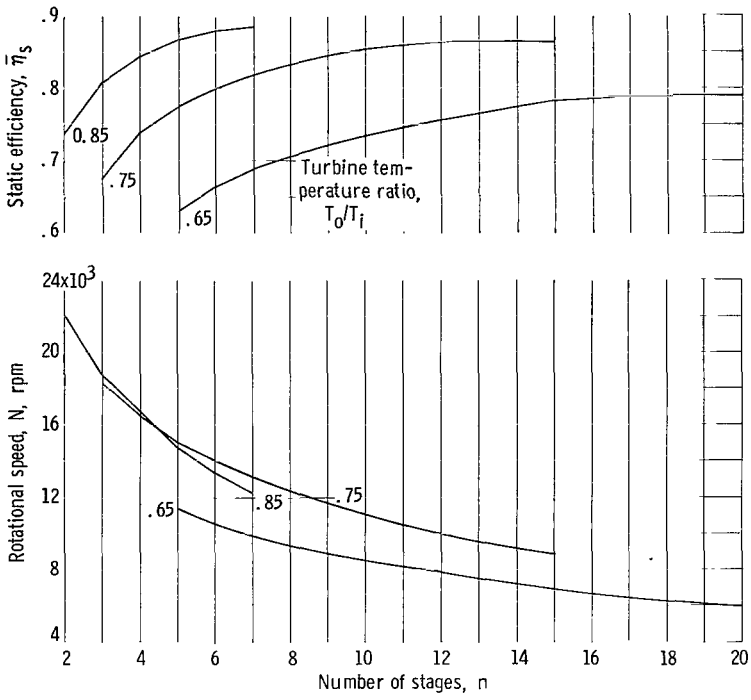

(b) Cross plot of efficiency and rotational speed trends.

Figure 9. - Concluded. Constant-blade-mean-section-diameter turbine characteristics as functions of turbine temperature ratio. (See table I for reference conditions.)

Since the efficiency reduction due to moisture could be expected to decrease as turbine temperature ratio is increased, overall turbine efficiency would increase faster than indicated in figure 9(a).

For a fixed number of stages, increasing the turbine temperature ratio also increased the stage speed-work parameter and the first-stage blade height, while the rotational speed increased, reached a maximum, and then decreased. (Although not shown, the mean diameter of the solutions minimized where n was maximized.) The temperature ratio at which the rotational speed maximized was a function of the number of stages and increased as the number of stages decreased.

Changes in efficiency and rotational speed are compared in the cross plot figure 9(b). The obtainable maximum static efficiency (neglecting moisture effects) decreased with decreasing turbine temperature ratio. Also, considerably more stages were required to obtain a given level of efficiency as turbine temperature ratio was decreased; however, turbine tapering could be employed to reduce the number of required stages.

Selection of low turbine temperature ratios may penalize the system with reduced turbine performance and the complexity of many turbine stages.

Power level. - Since a change in generator power level is reflected in the turbine by a linear change in weight flow, it is reasonable to expect that turbine diameter and rotational speed should scale with a change in power level. That is, for any given turbine taper ratio and number of stages, the diameters should vary directly as the square root of the power level, while the rotational speed should vary inversely as the square root of the power level.

Turbine solutions were obtained over the range in generator power level from 1 to 10 megawatts at the reference conditions of table I. Within a ±2 percent variation and independent of number of stages and turbine taper ratio, the results correlated with the scaling procedure. Thus, for example, if a turbine design for a 1 megawatt generator output prescribed a last-stage mean diameter of 1 foot and a rotational speed of 20,000 rpm, then the similar turbine configuration at 10 megawatts of generator output would have a diameter

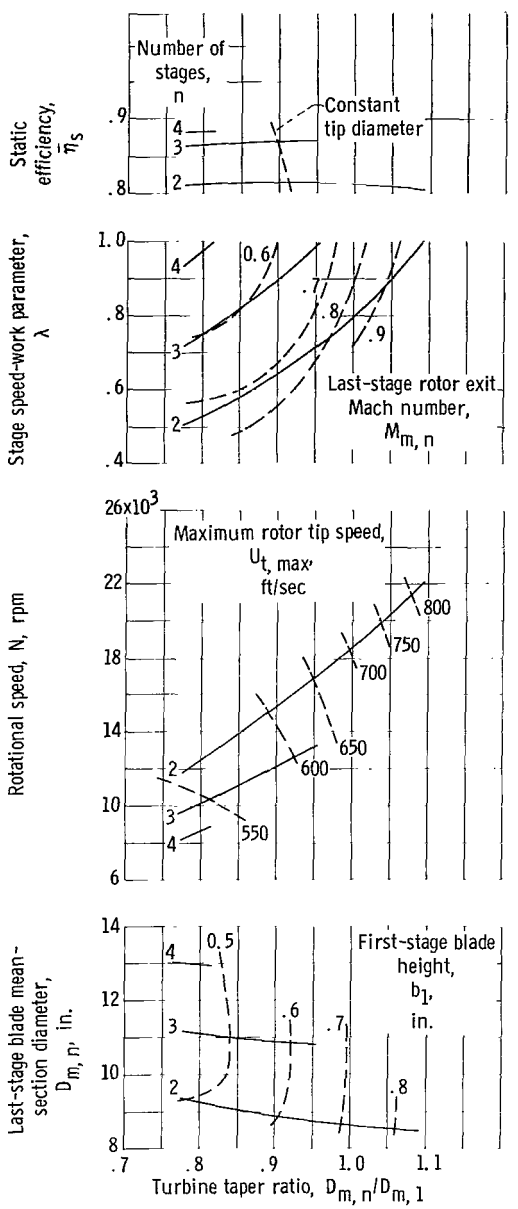

Figure 10. - Characteristics of cesium turbines. (See table I for reference conditions.)

of 3.16 feet (±0.06), while the rotational speed would be 6320 rpm (±126).

Working fluid. - Effects of taper ratio on turbine characteristics when cesium, rubidium, and sodium are used as working fluids are shown in figures 10 to 12, respectively.

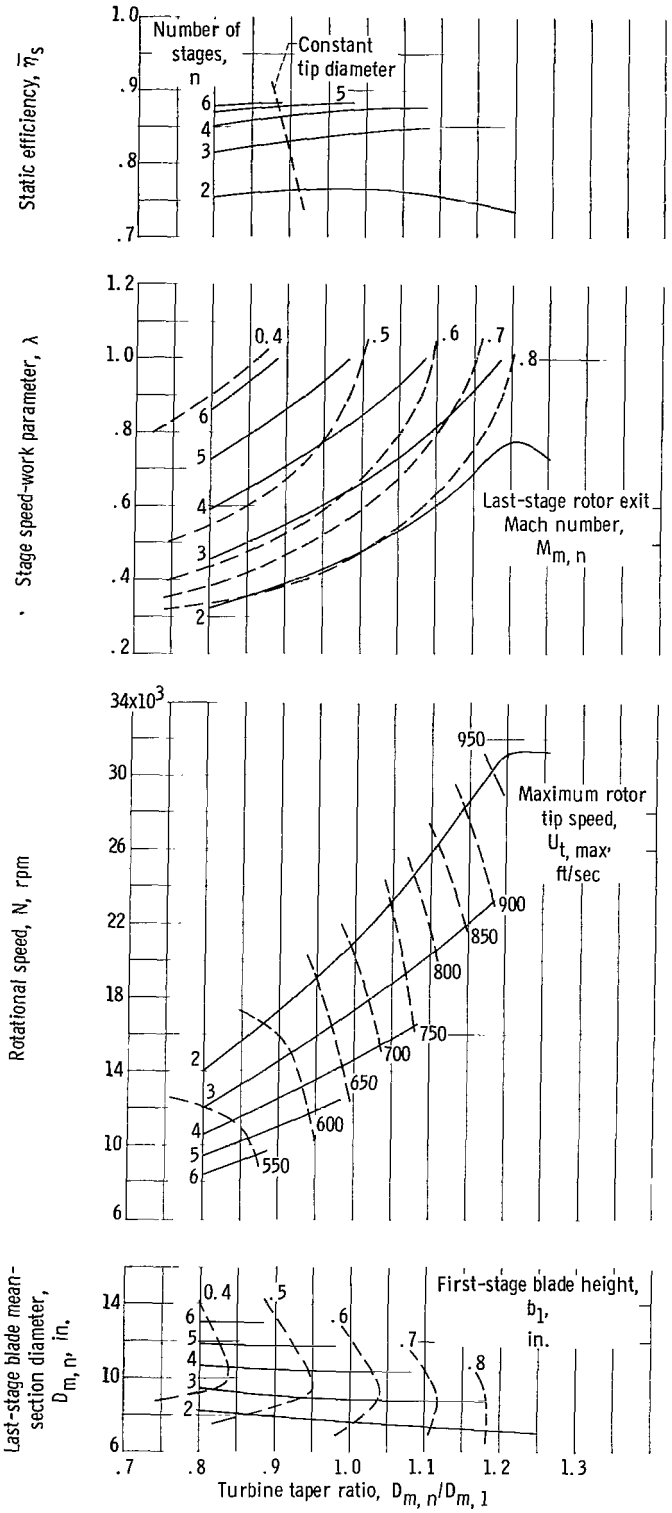

Figure 11. - Characteristics of rubidium turbines. (See table I for reference conditions.)

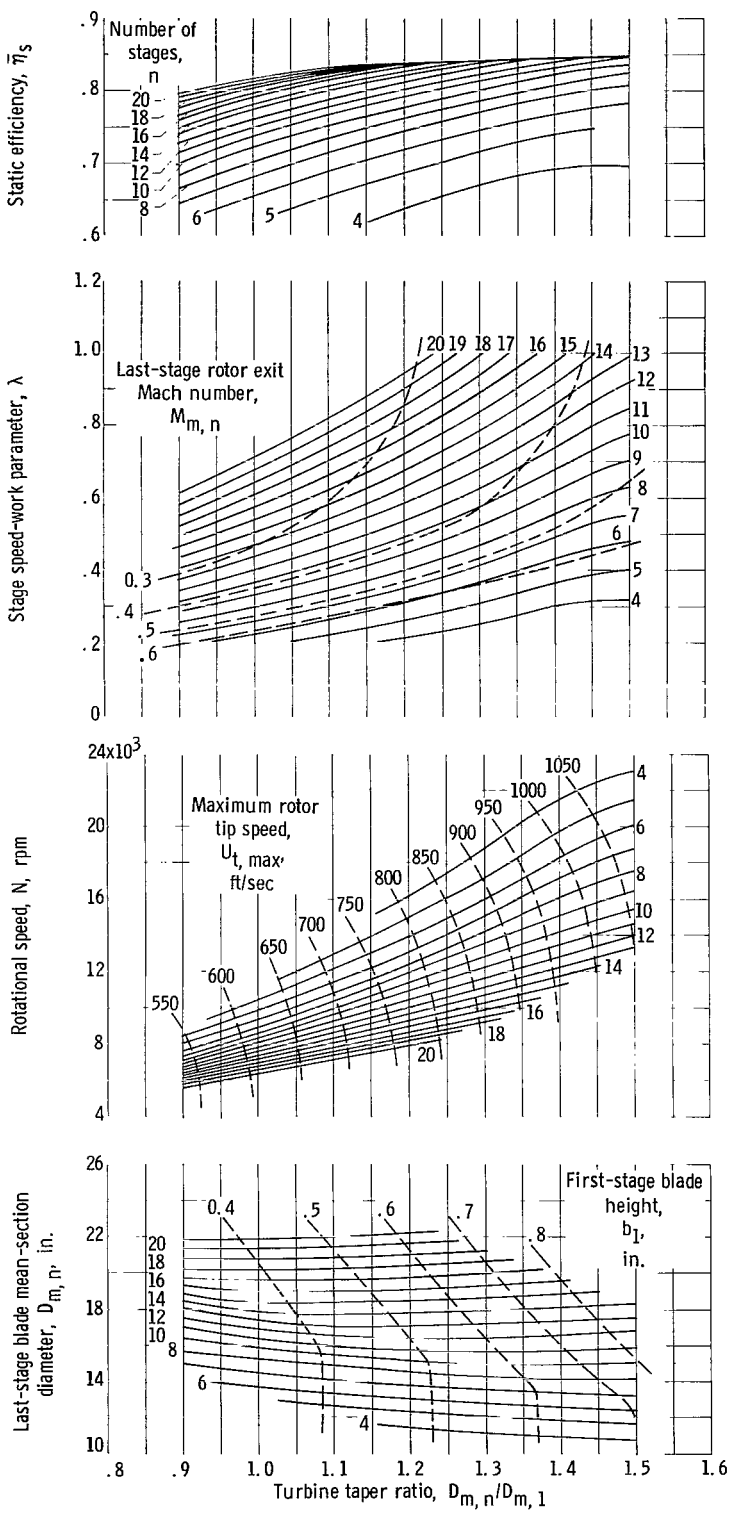

Figure 12. - Characteristics of sodium turbines. (See table I for reference conditions.)

The cesium solutions were characterized by the fewest number of stage solutions and very limited flexibility with respect to design variations. Three stages of nearly constant tip diameter ($D_{m,n}/D_{m,1}$ = 0.95) represented the highest obtainable efficiency with a reasonable turbine shape. This maximum efficiency solution was also characterized by a fairly reasonable first-stage blade height (about 0.6 in.) and the lowest level of rotor tip speed (about 640 ft/sec maximum) among the peak efficiency solutions of the four working fluids.

The rubidium solutions (fig. 11) were characterized by a few more number-of-stage solutions and a little more design flexibility than those for cesium. The constant-tip- and constant-mean-diameter solutions for any number of stages were near peak efficiency. Either six constant-tip-diameter stages or five nearly constant-mean-diameter stages ($D_{m,n}/D_{m,1}$ = 0.985) afforded maximum efficiency.

The sodium solutions (fig. 12) were characterized by four to twenty or more stages with large regions of design control with taper ratio. Up to the maximum taper ratio investigated (1.5), only the four- and five-stage solutions were approaching the shift in stress limitation from the first-stage disk. It may also be noted that the maximum efficiency level is 0.85 in figure 12. In general, it is felt that, if more stages and/or larger turbine taper

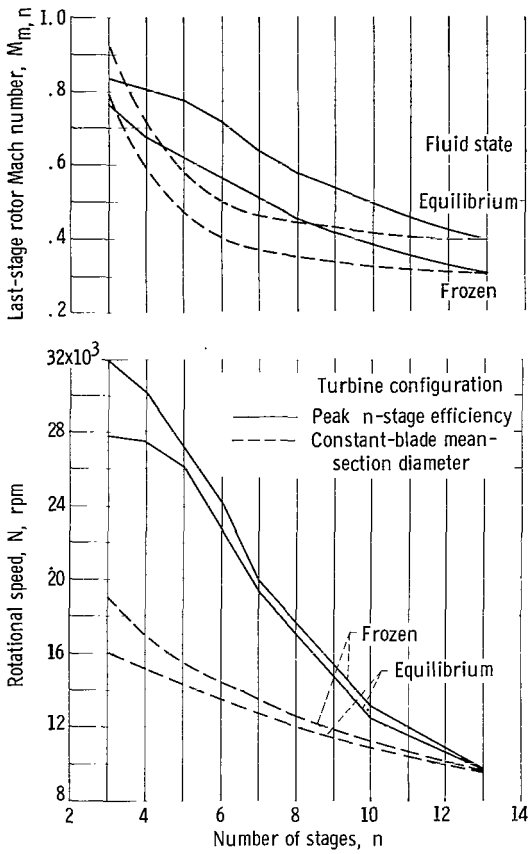

Figure 13. - Comparison of fluid state assumptions on turbine characteristics. (See table I for reference conditions.)

ratios were investigated, the obtainable static efficiency level would approach those obtained with the other working fluids (approximately 0.88).

In general, the number of stages required for peak efficiency decreased with increasing molecular weight of the working fluid (i.e., from sodium to potassium to rubidium to cesium), while the effectiveness of the turbine flow passage tapering in improving aerodynamic efficiency decreased. At a turbine inlet temperature of 2500° R, with sodium as the working fluid, 12 stages tapered by at least 50 percent would be required to attain maximum efficiency; while for potassium, 7 stages tapered by roughly 30 percent would be required, and 5 and 3, untapered stages would be required for rubidium and cesium, respectively.

On the other hand, it may also be advantageous to have the larger degree of freedom in choice of design rotational speed that would be available by the combined effect of tapering and stator exit angle previously exhibited for potassium turbine solutions.

Fluid state. - The effect of the "frozen" fluid state assumption of this analysis on Mach number level and rotational speed is compared with an "equilibrium" state in figure 13. Both constant-mean-diameter and tapered peak-efficiency configurations are compared. It can be seen that the frozen assumption resulted in lower Mach number levels (by about 0.1) and higher rotational speeds (by not more than 18 percent) as compared to the equilibrium results.

CONCLUSIONS

Axial-flow, alkali-metal vapor turbines have been investigated as one of the components in megawatt space electric powerplants. A parametric analysis has been conducted to determine the interactions of several design variables in obtaining maximum turbine efficiency. Efficiency reductions due to the presence of moisture were not included. The following conclusions were reached:

1. Turbine tapering (i.e., changing the ratio of last- to first-stage blade mean-section diameter) was an effective means for attaining maximum efficiency with a minimum number of stages. Turbine taper ratios for maximum efficiency decreased with increasing working fluid molecular weight. At an inlet

temperature of 2500° R, these solutions were characterized by the following:

(a) 12 stages for sodium, with a taper ratio of at least 1.5

(b) 7 stages for potassium, with a taper ratio of roughly 1.3

(c) 5 stages for rubidium, with a taper ratio of 0.985 (nearly constant mean diameter)

(d) 3 stages for cesium, with a taper ratio of 0.95 (nearly constant tip diameter)

2. Turbine tapering and/or small variations in stator exit angle permit a wider selection of design rotational speed, while still maintaining a desired level of efficiency.

3. Advantages of turbine tapering in reducing the number of stages required for nearly maximum efficiency decreased with decreased inlet temperature.

4. Selection of a low ratio of outlet to inlet temperature may penalize turbine performance.

Lewis Research Center
National Aeronautics and Space Administration
Cleveland, Ohio, August 20, 1964

APPENDIX A

SYMBOLS

A	annular flow area, sq in.
a	speed of sound, ft/sec
b	blade height, in.
C_p	vapor specific heat at constant pressure, Btu/(lb)(^oR)
c	axial blade chord, in.
D	diameter, in.
$D_{m,n}/D_{m,1}$	turbine taper ratio
g	acceleration due to gravity, 32.174 ft/sec^2
h	enthalpy, Btu/lb
J	mechanical equivalent of heat, 778.26 (ft)(lb)/Btu
M	Mach number
m	vapor molecular weight
N	rotational speed, rpm
N/N_k	ratio of rotational speed to n-stage constant-mean-diameter rotational speed
n	number of stages
P	power level, Mw
Re	Reynolds number
r	radius, in.
r_h/r_t	hub-to-tip radius ratio
S	entropy, Btu/(lb)(^oR)
T	temperature, ^oR
t_d	thickness of disk at rim, in.
U	wheel speed, ft/sec

V absolute velocity, ft/sec

W velocity relative to rotor blade, ft/sec

w weight flow, lb/sec

X quality of vapor

y_a thickness of disk at axis of rotation, in.

y_a/t_d disk taper ratio

α stator exit angle at blade mean-section radius, measured from axial direction, deg

β rotor angle at blade mean-section radius, measured from axial direction, deg

γ ratio of specific heats

Δ difference

η efficiency

λ stage speed-work parameter, $Um^2/gJ(\Delta h)$

μ vapor viscosity into turbine, lb/(ft)(sec)

ρ vapor density, lb/cu ft

ρ_{TZM} density of turbine material, 639 lb/cu ft

σ stress, psi

ψ stress correction factor for tapered blades

Subscripts:

a allowable

b blade

d disk

e equilibrium

g generator

h hub

i inlet

id	ideal
j	dummy variable referring to stage number, 1 to n
k	constant-blade mean-section diameter
l	liquid
m	blade mean section
max	maximum
n	last stage
o	outlet
p	peak
s	static
T	turbine
t	tip
v	vapor
x	axial component
θ	tangential component

Superscript:

$\bar{}$	overall

APPENDIX B

ANALYTICAL PROCEDURE

The investigation was programed for computation on an IBM 7094 digital machine. The working equations and the general approach are presented in this appendix.

Input Conditions

Input to the program included working fluid properties, assigned turbine requirements, and a series of constants. All working fluid properties with the exception of vapor viscosity were obtained from reference 5. The properties required for the turbine computation procedure were vapor density ρ, speed of sound a, and the ratio of specific heats γ as functions of temperature and single values of inlet vapor viscosity μ (obtained from ref. 6). Both "frozen" and "equilibrium" values (as defined in ref. 5) of the speed of sound and the ratio of specific heats were investigated. The equilibrium ratios of specific heats were calculated from the properties listed in reference 5 as

$$\gamma_e = \frac{C_{p,e}}{C_{p,e} - \frac{1.9865}{m_e}} \tag{B1}$$

Interpolation of a, γ, and ρ in the machine program was done by the Gregory-Newton method (ref. 7, p. 264) by using three forward differences. Because of the large rate of change of density with temperature, this property was interpolated logarithmically by using the Gregory-Newton method.

The assigned turbine requirements were inlet temperature T_i, temperature ratio T_o/T_i, overall specific work $\overline{\Delta h}$, weight flow w, and exit quality X_o. For each fluid and inlet temperature, those turbine temperature ratios that yield minimum specific radiator area (sq ft/kw) were determined from the method of reference 3 (modified Rankine cycle), but using an assumed generator efficiency of 0.9. In order to calculate the required turbine work and weight flow, the overall turbine efficiency was assumed to be 0.8. Then, the overall turbine work was evaluated from

$$\begin{aligned} \overline{\Delta h}_T &= \overline{\eta}_T (h_i - h_{o,id})_T \\ &= 0.8(h_i - h_{o,id}) \end{aligned} \tag{B2}$$

where

$$h_{o,id} = h_{o,v} - T_o(S_{o,v} - S_{i,v}) \tag{B3}$$

the turbine weight flow from

$$w = 949 \frac{P}{\eta_g \overline{\Delta h_T}} = 1053 \frac{P}{\overline{\Delta h_T}} \tag{B4}$$

and the turbine exit quality from

$$X_o = \frac{h_o - h_{o,l}}{h_{o,v} - h_{o,l}} \tag{B5}$$

For reference, these turbine working conditions are given in table II.

TABLE II. - TURBINE WORKING CONDITIONS

Inlet temperature, T_i, ^oR	Working fluid	Temperature ratio, T_o/T_i	Overall turbine work, $\overline{\Delta h_T}$, Btu/lb	Outlet quality, X_o	Specific weight flow, lb/(sec)(Mw)	Inlet viscosity, μ, lb/(ft)(sec)
2500	Sodium	0.772	302	0.854	3.49	1.53×10^{-5}
	Potassium	.776	150	.877	7.02	1.70
	Rubidium	.778	60.0	.889	17.5	2.03
	Cesium	.778	36.0	.896	29.3	2.16
2500	Potassium	0.65	245.5	0.801	4.29	1.70×10^{-5}
		.70	207.0	.831	5.08	
		.75	169.4	.861	6.21	
		.80	132.9	.891	7.92	
		.85	98.2	.919	10.71	
2400	Potassium	0.775	152	0.872	6.92	1.50×10^{-5}
2300	Potassium	.775	154	.869	6.83	1.47×10^{-5}

Other pertinent input quantities included the assumed turbine material density ρ_{TZM}, allowable stresses σ_a, blade mean-section stator exit angle α, last-stage hub-to-tip radius ratio $(r_h/r_t)_n$, turbine taper ratio $D_{m,n}/D_{m,1}$, and disk taper ratio limit $(y_a/t_d)_{max}$. Arbitrarily, a molybdenum-based alloy containing 0.45 percent titanium and 0.07 percent zirconium (TZM) has been assumed as the disk and blade material. Allowable stresses were determined from the data of reference 8 by extrapolating rupture stress on a Larson-Miller plot to 20,000 hours. In general, 50 percent of these extrapolated rupture stresses were used as the allowable stress. These were $\sigma_a = 9.8 \times 10^4$ pounds per square inch at 1600° R and $\sigma_a = 9.9 \times 10^3$ pounds per square inch at 2700° R with an assumed linear variation of the logarithm to the base 10 of the stresses between these temperatures.

Work-Speed Balance

The first portion of the calculation is to determine all combinations of n, λ, and N in the range $0.2 \leq \lambda \leq 1.0$ and $2 \leq n \leq 20$ that satisfy the overall turbine work requirement within the assumed allowable stresses. A

solution to a problem is initiated by setting $\lambda = 0.2$ and $n = 2$. An iterative procedure is then employed to find the compatible values of the axial components of velocity into the first- and last-stage rotors ($V_{x,i,1}$ and $V_{x,i,n}$, see fig. 14 for velocity diagram nomenclature) and rotational speed for the minimum value of the stage speed-work parameter.

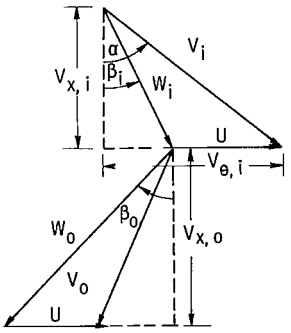

Figure 14. - Velocity diagram nomenclature.

Initially, arbitrary values are assigned to $V_{x,i,1}$ and $V_{x,i,n}$, and the temperature and quality of the working fluid into the last stage are estimated. Then, from the geometry, the absolute velocity into the first and last stage at the mean radius is given by

$$V_i = V_{x,i}\sqrt{1 + \tan^2 \alpha} \tag{B6}$$

Then, in order to correct to static flow conditions, the Mach numbers and the density ratios (assuming perfect gas relations) are evaluated from

$$M_i = \frac{\frac{V_i}{a}}{\sqrt{1 - \frac{\gamma-1}{2}\left(\frac{V_i}{a}\right)^2}} \tag{B7}$$

where a is the speed of sound corresponding to the total temperature T_i entering the stage in question, and

$$\left(\frac{\rho}{\rho_s}\right)_i = \left(1 + \frac{\gamma-1}{2} M_i^2\right)^{\frac{1}{\gamma-1}} \tag{B8}$$

The annular flow area required to pass only the vapor is calculated from

$$A = \frac{144 X_i w}{\rho_i V_{x,i}} \left(\frac{\rho}{\rho_s}\right)_i \tag{B9}$$

Since $(r_h/r_t)_n$ is specified as input to the problem, the last-stage radii follow from

$$\left.\begin{aligned} r_{t,n} &= \sqrt{\frac{A_n}{\pi\left[1 - \left(\frac{r_h}{r_t}\right)_n^2\right]}} \\ r_{h,n} &= r_{t,n}\left(\frac{r_h}{r_t}\right)_n \\ r_{m,n} &= \frac{r_{t,n} + r_{h,n}}{2} \end{aligned}\right\} \tag{B10}$$

The first-stage radii follow from the prescribed taper ratio $D_{m,n}/D_{m,1}$ and

$$\left.\begin{aligned} r_{m,1} &= \frac{r_{m,n}}{\frac{D_{m,n}}{D_{m,1}}} \\ r_{t,1} &= r_{m,1} + \frac{A_1}{4\pi r_{m,1}} \\ r_{h,1} &= r_{m,1} - \frac{A_1}{4\pi r_{m,1}} \end{aligned}\right\} \tag{B11}$$

Intermediate-stage radii are calculated proportionately between the first- and last-stage radii. In order to determine the radii of the disks at the rims, a mean axial chord is determined from

$$c = \frac{c_1 + c_n}{2} \tag{B12}$$

where

$$c_1 = \frac{r_{t,1} - r_{h,1}}{2} = \frac{b_1}{2}$$

$$c_n = \frac{r_{t,m} - r_{h,n}}{2} = \frac{b_n}{2}$$

with the arbitrary restriction that c_1 and c_n be equal to or greater than 1/2 inch. Then, since square rims were assumed (of width equal to c), the radii of the disks at the rims are calculated from

$$r_{d,j} = r_{h,j} - c \tag{B13}$$

where $j = 1, 2, \ldots, n$

Angular speed is now determined as the minimum value from among those calculated by assuming the blades and then the disks of each stage to be stress limited. The radial stress at the hub of tapered blades is given by (see ref. 9)

$$\sigma_b = \frac{\pi\psi\rho_{TZM}N^2A}{2(12)^4(30)^2g} \tag{B14}$$

Therefore, if the blades are stress limited,

$$N = 4320\sqrt{\frac{2g\sigma_a}{\pi\psi\rho_{TZM}A}} \tag{B15}$$

Conservatively, it was assumed that the steady-state temperature of the wheels was uniform and equal to the temperature of the vapor entering the stage. Hence, σ_a is evaluated for each stage at $T_{i,j}$. The stress level for a constant-stress disk with no temperature gradient is evaluated from (see ref. 9)

$$\sigma_d = \frac{\pi^2 \rho_{TZM} N^2 r_d^2}{2(12)^4(30)^2 g \ln\left(\frac{y_a}{t_d}\right)} \tag{B16}$$

Therefore, if a disk is stress limited, it attains the disk taper ratio limit $\left(\frac{y_a}{t_d}\right)_{max}$ assigned to the problem, and the rotational speed is

$$N = \frac{4320}{\pi}\sqrt{\frac{2g\sigma_a}{\rho_{TZM} r_d^2} \ln\left(\frac{y_a}{t_d}\right)_{max}} \tag{B17}$$

The next step in the procedure is to check the resulting first- and last-stage stator exit angles at the mean radius (α_1 and α_n) against those assigned by the problem. The stage speed-work parameter is defined (ref. 4) as

$$\lambda \equiv \frac{U_{m,j}^2}{gJ\,\Delta h_j} \tag{B18a}$$

and may also be written as

$$\lambda = \frac{U_m}{\Delta V_{\theta,m}} = \frac{\pi N r_m}{30(V_{\theta,m,i} - V_{\theta,m,o})} \tag{B18b}$$

Since λ is specified and N and r_m have been calculated, the change in the tangential velocity component for the first and last stage are computed from equation (B18b). Also, depending on the current value of λ, $V_{\theta,i}$ is found from

$$\left.\begin{aligned} V_{\theta,i} &= \left(\lambda + \frac{1}{2}\right)\Delta V_\theta \qquad \text{for } 0 \le \lambda \le 0.5 \\ V_{\theta,i} &= \Delta V_\theta \qquad \text{for } 0.5 \le \lambda \le 1.0 \end{aligned}\right\} \tag{B19}$$

Then,

$$\tan \alpha = \frac{V_{\theta,m,i}}{V_{x,i}} \tag{B20}$$

If either or both the first- and last-stage stator exit angles do not agree with the assigned values, then new axial components of the absolute velocity are computed as

$$V_{x,i} = \frac{V_{\theta,m,i}}{\tan \alpha} \tag{B21}$$

Before being iterated, the stage and total turbine work are calculated from

$$\left.\begin{aligned} \Delta h_j &= \frac{U_{m,j}^2}{gJ\lambda} \qquad j = 1, 2, \ldots, n \\ \overline{\Delta h_T} &= \sum_{j=1}^{n} \Delta h_j \end{aligned}\right\} \tag{B22}$$

and new values are computed for $T_{i,n}$ and $X_{i,n}$. The change in temperature and quality across a turbine stage was assumed to be proportional to the stage work. Therefore,

$$\left.\begin{aligned} T_{i,n} &= T_{o,n} + \left[\frac{\Delta h_n}{\overline{\Delta h_T}}\right]\overline{\Delta T}_T \\ X_{i,n} &= X_{o,n} + \left[\frac{\Delta h_n}{\overline{\Delta h_T}}\right]\overline{\Delta X}_T \end{aligned}\right\} \tag{B24}$$

The procedure now goes back to equation (B6) and iterates until the correct values of $V_{x,i,1}$, $V_{x,i,n}$, and n are obtained for the assumed $\lambda = 0.2$. Now if the total turbine work is greater than the required turbine work, a new value of λ is calculated as the current work divided by the required work times the previous value of λ. The procedure again reverts to equation (B6) and iterates until the turbine work equals the requirement. On the other hand, if the current turbine work for $\lambda = 0.2$ is less than the required amount, then no solution is possible and the number of stages is increased by one. The calculation then repeats by assuming arbitrary values of $V_{x,i,1}$ and $V_{x,i,n}$ and with the new value for n goes back to equation (B6).

Once the work and speed requirements are balanced as described in this section, the calculation continues as in the following section. After the entire calculation for a particular n is completed, a new calculation is made for $n + 1$. A problem is terminated either when $\lambda > 1.0$ or $n > 20$.

Efficiency Estimation

The approach of Stewart (ref. 4) was used but modified to include the relatively small effect of reheat (enthalpy level). The entire procedure is included for the reader's convenience. Stage total and static efficiencies are given, respectively, in reference 4 as

$$\eta = \frac{\Delta h}{\Delta h_{id}} = \frac{\lambda}{\lambda + \frac{1}{2}A} \tag{B25}$$

and

$$\eta_s = \frac{\Delta h}{\Delta h_{id,s}} = \frac{\lambda}{\lambda + \frac{1}{2}(A + B)} \tag{B26}$$

where

$$A = \frac{0.4 Re^{-1/5}}{\cot \alpha} (C + 2D) \tag{B27}$$

with the Reynolds number given by

$$Re = \frac{12w}{\mu r_{m,1}} \tag{B28}$$

and the expressions B, C, D evaluated in table III.

TABLE III. - VARIATION OF EFFICIENCY TERMS

WITH STAGE SPEED-WORK PARAMETER

$0 \leq \lambda \leq 0.5$	$0.5 \leq \lambda \leq 1.0$
$B = \left(\frac{V_{x,o}}{V_{x,i}}\right)^2 \cot^2\alpha\left(\lambda + \frac{1}{2}\right)^2 + \left(\lambda - \frac{1}{2}\right)^2$	$B = \left(\frac{V_{x,o}}{V_{x,i}}\right)^2 \cot^2\alpha$
First stage:	
$C = (1 + 2 \cot^2\alpha)\left(\lambda + \frac{1}{2}\right)^2$	$C = 1 + 2 \cot^2\alpha$
Other stages:	
$C = 2(1 - \lambda)\left[(1 + 2 \cot^2\alpha)\left(\lambda + \frac{1}{2}\right)^2 + \left(\lambda - \frac{1}{2}\right)^2\right]$	----------
$D = 2 \cot^2\alpha\left(\lambda + \frac{1}{2}\right)^2 + \frac{1}{2}$	$D = 2 \cot^2\alpha + (1 - \lambda)^2 + \lambda^2$

Overall static efficiency may be expressed as

$$\overline{\eta}_s = \frac{\overline{\Delta h}}{\overline{\Delta h}_{id,s}} \quad \frac{\sum_{j=1}^{n} \Delta h_j}{\overline{\Delta h}_{id,s}} \tag{B29}$$

Also,

$$\overline{\Delta h}_{id,s} = \sum_{j=1}^{n-1} \Delta h_j + \Delta h_{id,s,n} + T_{o,s,n}(S_{i,n} - S_{i,1}) \tag{B30}$$

now,

$$\Delta h_{id,s,n} = \frac{1}{\eta_{s,n}} \Delta h_n \tag{B31}$$

and

$$S_{i,n} - S_{i,1} = \sum_{j=1}^{n=1} (S_{o,j} - S_{i,j}) \tag{B32}$$

with

$$\left(\Delta h_{id} - \Delta h\right)_j = T_{o,j}(S_{o,j} - S_{i,j}) \tag{B33}$$

or

$$S_{i,n} - S_{i,1} = \sum_{j=1}^{n-1} \frac{1}{T_{o,j}} \left(\frac{1}{\eta_j} - 1\right) \Delta h_j \tag{B34}$$

Combining equations (B29) to (B31) and (B34) yields the overall turbine static efficiency as

$$\overline{\eta_s} = \frac{\sum_{j=1}^{n} \Delta h_j}{\sum_{j=1}^{n-1} \Delta h_j + \frac{1}{\eta_{s,n}} \Delta h_n + T_{o,s,n} \sum_{j=1}^{n-1} \frac{1}{T_{o,j}} \left(\frac{1}{\eta_j} - 1\right) \Delta h_j} \tag{B35}$$

The value of the static exit temperature is calculated from the ideal gas relation:

$$T_{o,s,n} = T_{o,n}\left(1 + \frac{\gamma - 1}{2} M_{o,n}^2\right)^{-1} \tag{B36}$$

REFERENCES

1. Bolan, Peter: Parametric Studies Report - Advanced Nuclear Electric Power Generator System Study - Rankine Cycle Nuclear Space Powerplant. Rep. PWA-2232, Pratt and Whitney Aircraft, Aug. 26, 1963.

2. Moffitt, Thomas P., and Klag, Frederick W.: Analytical Investigation of Cycle Characteristics for Advanced Turboelectric Space Power Systems. NASA TN D-472, 1960.

3. Glassman, Arthur J., and Futral, S. M.: Analytical Study of Turbine-Geometry Characteristics for Alkali-Metal Turboelectric Space Power Systems. NASA TN D-1710, 1963.

4. Stewart, Warner L.: A Study of Axial-Flow Turbine Efficiency Characteristics in Terms of Velocity Diagram Parameters. Paper 61-WA-37, ASME, 1961.

5. Meisl, C. J., and Shapiro, A.: Thermodynamic Properties of Alkali Metal Vapors and Mercury. R60FPD358-A, General Electric Co., Nov. 9, 1960.

6. Weatherford, W. D., Jr., Tyler, John C., and Ku, P. M.: Properties of Inorganic Energy-Conversion and Heat-Transfer Fluids for Space Applications. TR 61-96, WADD, 1961.

7. Burington, Richard S.: Handbook of Mathematical Tables and Formulas. Third ed., McGraw-Hill Book Co., Inc., 1948.

8. Houck, J. A.: Physical and Mechanical Properties of Commercial Molybdenum-Base Alloys. DMIC Rep. 140, Defense Metals Info. Center, 1960.

9. LaValle, Vincent L., and Huppert, Merle C.: Effects of Several Design Variables on Turbine-Wheel Weight. NACA TN-1814, 1949.

"The aeronautical and space activities of the United States shall be conducted so as to contribute . . . to the expansion of human knowledge of phenomena in the atmosphere and space. The Administration shall provide for the widest practicable and appropriate dissemination of information concerning its activities and the results thereof."

—NATIONAL AERONAUTICS AND SPACE ACT OF 1958

NASA SCIENTIFIC AND TECHNICAL PUBLICATIONS

TECHNICAL REPORTS: Scientific and technical information considered important, complete, and a lasting contribution to existing knowledge.

TECHNICAL NOTES: Information less broad in scope but nevertheless of importance as a contribution to existing knowledge.

TECHNICAL MEMORANDUMS: Information receiving limited distribution because of preliminary data, security classification, or other reasons.

CONTRACTOR REPORTS: Technical information generated in connection with a NASA contract or grant and released under NASA auspices.

TECHNICAL TRANSLATIONS: Information published in a foreign language considered to merit NASA distribution in English.

TECHNICAL REPRINTS: Information derived from NASA activities and initially published in the form of journal articles.

SPECIAL PUBLICATIONS: Information derived from or of value to NASA activities but not necessarily reporting the results of individual NASA-programmed scientific efforts. Publications include conference proceedings, monographs, data compilations, handbooks, sourcebooks, and special bibliographies.

Details on the availability of these publications may be obtained from:

SCIENTIFIC AND TECHNICAL INFORMATION DIVISION

NATIONAL AERONAUTICS AND SPACE ADMINISTRATION

Washington, D.C. 20546